

EFFECTS OF AN INCLINED CENTRED CONDUCTOR ON MHD NATURAL AND FORCED CONVECTION WITHIN A HEATED WAVY CHAMBER.

Abstract: The study of the effect of hall and ion slip on an inclined conductor on MHD natural and forced convection in a heated wavy chamber with a constant transversal magnetic field applied. The governing momentum and energy equation were solved by applying finite central scheme approximation and the resulting partial difference equations were solved by MATLAB software. The study showed that an increased heat absorption coefficient lowers the surface heat transfer thus lowering the flow rate. An increase in Rayleigh number increases the flow rate while an increase in the angle of inclination of the conductor increases the buoyancy force component thereby increasing the

flow rate. The results further showed that the flow rate became higher at an inclination angle of 90°. In addition, the results also showed that an increase in Hartmann increases the flow rate. The Hartmann number, Rayleigh number, and Absorption coefficient are analytically discussed and represented in tables and graphical profiles for flow velocity and temperature profile due to engineering demand. This current study has a direct application in the development of MHD-propelled vessels in the marine and spacecraft department.

Nomenclature

ω Angle of inclination.

B_0 Magnetic field strength

g Gravitational field strength.

u, v Velocity components in x and y direction respectively (m/s).

U, V Dimensionless velocity components along x and y axis.

T Thermodynamic temperature (Kelvin)

x, y Cartesian coordinates.

Pr Prandtl number

Rar Thermal Rayleigh number

Gr Grashof number

f Density (kg/m^3)

Re Reynolds number

P Static pressure (N/m^2)

Nu Nusselt number

T Thermodynamic temperature.

Ha Hartmann Number

Ne Buoyancy ratio

Abbreviations.

MHD Magneto-Hydrodynamic

CDS Central Difference Scheme

PDE Partial Differential Equation

Greek symbols.

α Thermal diffusivity (m^2/s)

σ Electrical conductivity (Ohm-metre)

k Thermal conductivity (W/M/K)

ϕ Absorption coefficient (1/cm)

β Fluid thermal expansion coefficient (1/K)

1. INTRODUCTION

Magneto hydrodynamic flow, which is the mass transfer of electrically conductive fluids within a magnetic field, is of vital importance both internationally and locally in the marine and aircraft depart among other sectors of engineering where it's gained massive application. In the Department of Marine and Aircraft, many researchers have tried to solve the problem. As charges flow through a magnetic field,

they give rise to some thrust force whose magnitude depends on the angle of inclination between the two fields (Flemings' 19th C). The force experienced between a conductive fluid and a magnetic field during an MHD convective flow can be used to develop vessels that are non-mechanical and easier to operate, non-polluting since they don't use combustible fuel as their propelling mechanism. This

force depends on many factors that this study has looked at and is found to be acting perpendicularly in the direction of the two fields. It is for this reason that the MHD convective flow knowledge becomes relevant to the marine and spacecraft department since the vessels developed are

Nasrin (2011) studied the effects of a conducting obstacle centered on MHD combined convection in a wavy chamber. The result showed that the Richardson number (Ri) and the diameter (D) of the

over an upright permeable plate with an induced magnetic field. The results obtained showed that the velocity profile decreases with an increase in the Prandtl number, magnetic parameter (m), and Schmidt number (Sc). Roizaini *et al.* (2020), investigated magnetic field effects on mixed convection heat transfer in a lid-driven rectangular cavity. The result of the study showed that the Hartmann number has a significant effect on the convective current. Arash Karimipour *et al.* (2020), investigated the magnetic field influence on combined convection heat transfer in a lid-driven rectangular enclosure. The results of the study showed that Hartmann number significantly affects the fluid flow structure

very fast, easy to maneuver, economical, and environmentally friendly to operate, unlike the mechanical vessels. Therefore, how to increase the induced force during MHD flow has been the basis of most studies.

conducting obstacle strongly affect the flow phenomenon.

Khantun *et al.* (2018), numerically investigated the magnetohydrodynamic free convection fluid flow

and temperature field. Absana *et al.* (2021) investigated a two-dimensional unsteady MHD free convection flow over a vertical plate in the presence of radiation. The results of their study showed that the velocity profile of the flow decreases with an increase in radiative parameters while the velocity profiles reduced with an increase in the Prandtl number. From the above literature, it can be seen that there is no significant information on the effect of the angle of inclination of a centered conductor on MHD free and forced convection. The current study addresses this problem. The specific objectives of the study are:

- i. To formulate a mathematical model for the effects of an inclined

conductor on MHD natural and forced convection in a heated wavy chamber.

- ii. To determine the effect of the angle of inclination on temperature distribution.
- iii. To determine the influence of magnetic field on temperature distribution profile.
- iv. To determine the effects of flow parameters on temperature and velocity profile distribution.

2. Model Specification.

The set-up below consists of a two-dimensional lid-driven rectangular chamber of length P . The upper and lower parts of the cavity are insulated, the left lid is at a uniform velocity and the temperature T_i (20°C), while the right wall with a temperature T_h (100°C). The conductor is tilted through an angle (ω) for ($30^\circ \leq \omega \leq 90^\circ$) along the horizontal axis within a conductive fluid taken as the air of ($Pr = 0.71$). A constant magnetic field of strength B_o is applied in the horizontal direction to the sidewalls of the chamber

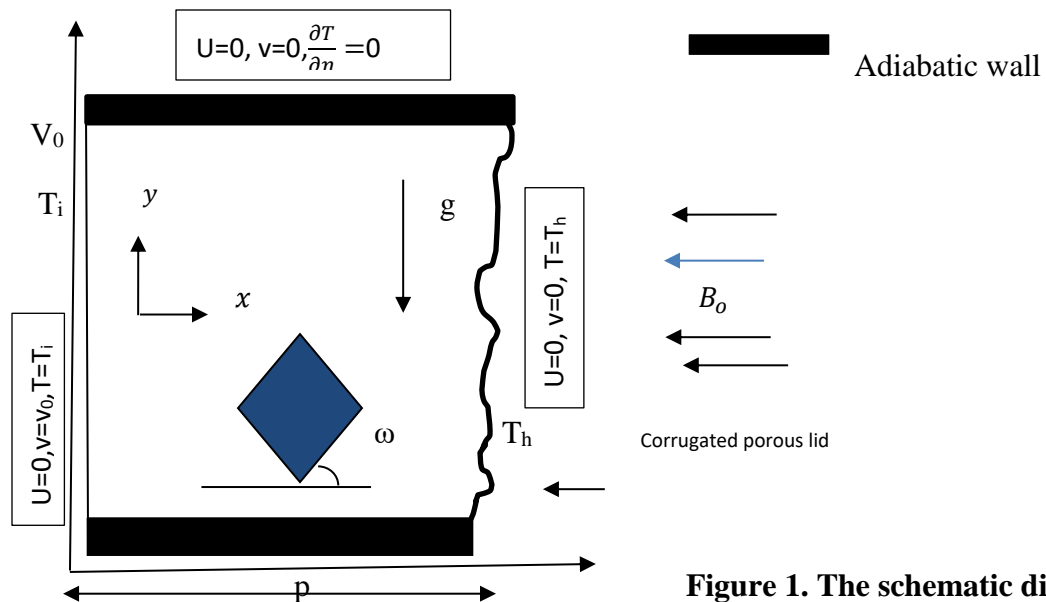


Figure 1. The schematic diagram.

T is the temperature, and B_0 is the external magnetic field strength.

2.1. Assumptions.

To solve and analyze this occurrence, the following assumptions are made:

- i. The flow is steady, laminar, 2-D, and incompressible.
- ii. The earth's magnetic effects are negligible
- iii. There is no radiation effect.
- iv. The magnetic effect is only experienced in the horizontal direction.
- v. The magnetic field meets the centered conductor perpendicularly.
- vi. There is no magnetic dissipation since the external magnetic field is a mono-pole with no other magnetic field interaction.

3. Mathematical formulation

The flow is assumed to be laminar, steady, and incompressible and that magnetic effect only acts horizontally.

3.1. Natural Convection.

The specific momentum equation for this case will be obtained by considering Newton's second law. The external forces acting on the fluid in this case are the buoyancy and magnetic force.

Equation along x-axis

$$u \frac{\partial u}{\partial x} + v \frac{\partial u}{\partial y} = -\frac{1}{\rho} \frac{\partial p}{\partial x} + v \left[\frac{\partial^2 u}{\partial x^2} + \frac{\partial^2 u}{\partial y^2} \right] + \sin \omega g \beta_T [T - T_c] \quad (1)$$

Equation along y-axis

$$u \frac{\partial v}{\partial x} + v \frac{\partial v}{\partial y} = -\frac{1}{\rho} \frac{\partial p}{\partial y} + v \left[\frac{\partial^2 v}{\partial x^2} + \frac{\partial^2 v}{\partial y^2} \right] + \cos \omega g \beta_T [T - T_c] - \frac{k \sigma \beta_0^2 v}{\rho} \quad (2)$$

Energy equation

$$u \frac{\partial T}{\partial x} + v \frac{\partial T}{\partial y} = \alpha \left[\frac{\partial^2 T}{\partial x^2} + \frac{\partial^2 T}{\partial y^2} \right] + \frac{Q_0}{\rho C_p} (T - T_c) \quad (3)$$

3.2. Forced Convection.

In this type of convection, there is a mass movement or fluid movement due to an external forcing condition.

Momentum along x-axis

$$u \frac{\partial u}{\partial x} + v \frac{\partial u}{\partial y} = \nu \frac{\partial^2 u}{\partial x^2} + \sin \omega \quad (4)$$

Momentum along the y-axis.

$$u \frac{\partial v}{\partial x} + v \frac{\partial v}{\partial y} = \nu \frac{\partial^2 v}{\partial y^2} + \cos \omega - \frac{k\sigma\beta_0^2 \nu}{\rho} \quad (5)$$

Energy equation.

$$u \frac{\partial T}{\partial x} + v \frac{\partial T}{\partial y} = \alpha \left[\frac{\partial^2 T}{\partial x^2} + \frac{\partial^2 T}{\partial y^2} \right] + \frac{Q_0}{\rho C_P} (T - T_c) \quad (6)$$

Introducing initial boundary conditions.

With initial boundary conditions:

$u = 0, v = v_0, T = T_i$ vertical walls

At horizontal wall: $u = 0, v = 0, \frac{\partial T}{\partial n} = 0$

At the wavy surface: $u = 0, v = 0, T = T_n$

At the solid-fluid interface $\left[\frac{\delta T}{\delta n} \right]_{fluid} = \frac{K_s}{K} \left(\frac{\delta T}{\delta n} \right)_{solid}$

The rate of heat transfer on the wavy wall is expressed in terms of Nusselt number

$$\overline{Nu} = \frac{\text{Convective heat transfer}}{\text{Conductive heat transfer}} = \frac{h}{K/L} = \frac{hl}{K} = \frac{\partial T}{\partial n} L$$

Introducing non-dimensional numbers:

$$X = \frac{x}{L}, Y = \frac{y}{L}, U = \frac{UL}{\alpha}, V = \frac{vL}{\alpha}, Pr = \frac{\rho L^2}{\mu \alpha}$$

$$\theta = \frac{T-T_c}{T_h-T_c}, Pr = \frac{\nu}{\alpha}, \alpha = \frac{K}{\rho c_p}, \sigma = \frac{\rho L^2}{\mu}$$

$$Ha^2 = \frac{\sigma B_0^2 L^2}{\mu}, Ra = \frac{g \beta L^3 (T_n - T_c) Pr}{\nu^2}, \sigma = \frac{\rho^2 \alpha}{L^2}, \alpha = \frac{K}{\rho c_p}$$

Momentum along x-axis

$$U \frac{\partial U}{\partial X} + V \frac{\partial U}{\partial Y} = -\frac{\partial P}{\partial X} + Pr \left[\frac{\partial^2 U}{\partial X^2} + \frac{\partial^2 U}{\partial Y^2} \right] + \sin \omega (Ra Pr [\theta - N_c]) \quad (7)$$

Equation along y-axis

$$U \frac{\partial V}{\partial X} + V \frac{\partial V}{\partial Y} = -\frac{\partial P}{\partial Y} + Pr \left[\frac{\partial^2 V}{\partial X^2} + \frac{\partial^2 V}{\partial Y^2} \right] + \cos \omega [Ra Pr (\theta - N_c) - Ha^2 Pr V] \quad (8)$$

Energy Equation.

The specific energy equation is obtained from the first law of Thermodynamics where Φ is the heat absorption coefficient.

$$U \frac{\partial \theta}{\partial X} + V \frac{\partial \theta}{\partial Y} = \left[\frac{\partial^2 \theta}{\partial X^2} + \frac{\partial^2 \theta}{\partial Y^2} \right] + \Phi \theta \quad (9)$$

FORCED CONVECTION

The dimensionless equation for this case becomes:

Equation along x-axis

$$U \frac{\partial U}{\partial X} + V \frac{\partial U}{\partial Y} = Pr \left[\frac{\partial^2 U}{\partial X^2} \right] + \sin \omega \quad (10)$$

Equation along y-axis

$$U \frac{\partial V}{\partial X} + V \frac{\partial V}{\partial Y} = \text{Pr} \left[\frac{\partial^2 V}{\partial Y^2} \right] + \cos \omega - Ha^2 \text{Pr} V \quad (11)$$

4. Method of solution

The problem under investigation generates partial differential equations whose solutions are to be determined using the finite difference approach. The momentum and energy equations are solved using the Finite central scheme technique. All four nodes (which are obtained from a uniform mesh of square concerning the central node) of velocity components U and V and temperature θ are the basic unknowns. The resulting pairs of linear simultaneous equations are then solved by MATLAB simulation software under a set of boundary conditions.

Discretization of Momentum Equation along the axis

We consider the Momentum Equation along the axis (7) and use it to investigate the fluid velocity profiles. For the central scheme (CDS), the values, U_x, U_y, U_{xx} and U_{yy} are replaced by the central difference approximation.

$$u \left(\frac{U_{i+1,j} - U_{i-1,j}}{2\Delta x} \right) + v \left(\frac{U_{i,j+1} - U_{i,j-1}}{2\Delta y} \right) = \left(\frac{U_{i+1,j} - 2U_{i,j} + U_{i-1,j}}{(\Delta x)^2} + \frac{U_{i,j+1} - 2U_{i,j} + U_{i,j-1}}{(\Delta y)^2} \right) + \sin \omega (Ra_T \text{Pr} (\theta - N_c)) \quad (12)$$

Take $U = V = N_c = \theta = 1$, multiply both sides by $2(\Delta x)$ and let $\text{Pr} = 0.71$, and take $\Delta x = \Delta y = 0.1$ on a square mesh into equation (12) we get the scheme;

$$0.86U_{i+1,j} + 8U_{i,j} - 1.14U_{i-1,j} = -0.86U_{i,j+1} + 1.14U_{i,j-1} + \sin \omega (Ra_T \text{Pr} (\theta - N_c)) \quad (13)$$

Taking $i = 1, 2, 3, \dots, 5$ and $j = 1$ we form the following systems of linear algebraic equations,

With initial and boundary conditions $U_{i,0} = U_{0,j} = 1$ $U_{i,2} = 0$ respectively, the above algebraic equations (13) can be written in matrix form as;

$$\begin{bmatrix} 8 & 0.86 & 0 & 0 & 0 \\ -1.4 & 8 & 0.86 & 0 & 0 \\ 0 & -1.4 & 8 & 0.86 & 0 \\ 0 & 0 & -1.4 & 8 & 0.86 \\ 0 & 0 & 0 & -1.4 & 8 \end{bmatrix} \begin{bmatrix} U_{1,1} \\ U_{2,1} \\ U_{3,1} \\ U_{4,1} \\ U_{5,1} \end{bmatrix} = \begin{bmatrix} 0.14 + 0.7 \sin \omega Ra_T \\ 0.07 + 0.7 \sin \omega Ra_T \\ 0.07 + 0.7 \sin \omega Ra_T \\ 0.07 + 0.7 \sin \omega Ra_T \\ 0.07 + 0.7 \sin \omega Ra_T \end{bmatrix} \quad (14)$$

We use equation (14) to investigate the effects of ωRa_T on the horizontal fluid velocity profile.

Discretization of Momentum Equation along y-axis

We consider Momentum Equation along y-axis (8) and use it to investigate the fluid velocity profiles. For the central scheme (CDS), the values, V_x, V_y, V_{xx} and V_{yy} are replaced by the central difference approximation. On substituting these values into Equation (8), it gives;

$$u \left(\frac{V_{i+1,j} - V_{i-1,j}}{2\Delta x} \right) + v \left(\frac{V_{i,j+1} - V_{i,j-1}}{2\Delta y} \right) = \left(\frac{V_{i+1,j} - 2V_{i,j} + V_{i-1,j}}{(\Delta x)^2} + \frac{V_{i,j+1} - 2V_{i,j} + V_{i,j-1}}{(\Delta y)^2} \right) + \cos \omega (Ra_T \Pr (\theta - N_c)) - 0.7 Ha^2 V_{i,j} \quad (15)$$

Take $U = V = N_c = \theta = 1$, multiply both sides by $2(\Delta x)$ and let $\Pr = 0.71$ and take $\Delta x = \Delta y = 0.1$ on a square mesh into equation (15) we get the scheme;

$$0.86V_{i+1,j} + (8 + Ha^2)V_{i,j} - 1.14V_{i-1,j} = -0.86V_{i,j+1} + 1.14V_{i,j-1} + \cos \omega (Ra_T \Pr (\theta - N_c)) \quad (16)$$

Taking and $i = 1,2,3,\dots,5$ and $j = 1$ we form the following systems of linear algebraic equations and with initial and boundary conditions $V_{i,0} = V_{0,j} = 1$ and $V_{i,2} = 0$ respectively, the above equation in its matrix form comes to:

$$\begin{bmatrix} (8 + Ha^2) & 0.86 & 0 & 0 & 0 \\ -1.4 & (8 + Ha^2) & 0.86 & 0 & 0 \\ 0 & -1.4 & (8 + Ha^2) & 0.86 & 0 \\ 0 & 0 & -1.4 & (8 + Ha^2) & 0.86 \\ 0 & 0 & 0 & -1.4 & (8 + Ha^2) \end{bmatrix} \begin{bmatrix} V_{1,1} \\ V_{2,1} \\ V_{3,1} \\ V_{4,1} \\ V_{5,1} \end{bmatrix} = \begin{bmatrix} 0.14 + 0.7 \cos \omega Ra_T \\ 0.07 + 0.7 \cos \omega Ra_T \\ 0.07 + 0.7 \cos \omega Ra_T \\ 0.07 + 0.7 \cos \omega Ra_T \\ 0.07 + 0.7 \cos \omega Ra_T \end{bmatrix} \quad (17)$$

We use equation (17) to investigate the effects of Ha^2 , ω and Ra_T on the vertical fluid velocity profile.

Discretization of Energy Equation

We consider Energy Equation (9) and use it to investigate the fluid temperature distribution. For the central scheme (CDS), the values, $\theta_x, \theta_x, \theta_{xx}$ and θ_{yy} are replaced by central difference approximation.

When these values are substituted into Equation (9), we get;

$$u \left(\frac{\theta_{i+1,j} - \theta_{i-1,j}}{2\Delta x} \right) + v \left(\frac{\theta_{i,j+1} - \theta_{i,j-1}}{2\Delta y} \right) = \left(\frac{\theta_{i+1,j} - 2\theta_{i,j} + \theta_{i-1,j}}{(\Delta x)^2} + \frac{\theta_{i,j+1} - 2\theta_{i,j} + \theta_{i,j-1}}{(\Delta y)^2} \right) + \Phi \theta_{i,j} \quad (18)$$

Take, multiply both sides by $2(\Delta x)$ and let $Pr = 0.71$ and take $\Delta x = \Delta y = 0.1$ on a square mesh into equation (18) we get the scheme;

$$-19\theta_{i+1,j} + (80 - 0.2\Phi)\theta_{i,j} - 21\theta_{i-1,j} = 19\theta_{i,j+1} + 21\theta_{i,j-1} \quad (19)$$

Taking and $i = 1, 2, 3, \dots, 5$ and $j = 1$ we form the following systems of linear algebraic equations and with initial boundary conditions and with initial and boundary conditions $\Theta_{i,0} = \Theta_{0,j} = 1$ and $\Theta_{i,2} = 0$ respectively, the above algebraic equation in its matrix form becomes:

$$\begin{bmatrix} (8 - 0.2\Phi) & 0.86 & 0 & 0 & 0 \\ -1.4 & (8 - 0.2\Phi) & 0.86 & 0 & 0 \\ 0 & -1.4 & (8 - 0.2\Phi) & 0.86 & 0 \\ 0 & 0 & -1.4 & (8 - 0.2\Phi) & 0.86 \\ 0 & 0 & 0 & -1.4 & (8 - 0.2\Phi) \end{bmatrix} \begin{bmatrix} \theta_{1,1} \\ \theta_{2,1} \\ \theta_{3,1} \\ \theta_{4,1} \\ \theta_{5,1} \end{bmatrix} = \begin{bmatrix} 420 \\ 210 \\ 210 \\ 210 \\ 210 \end{bmatrix} \quad (20)$$

We use equation (20) to investigate the effects of Φ , on the temperature distribution.

The next chapter details the results obtained for the effects of ω , Φ and Ra_T on the horizontal, vertical fluid velocity profiles and temperature distribution. The results are presented in tables and discussed graphically.

Code validation

The outcome of the present numerical code is pegged against the numerical result of B.A Odongo *et.al* (2021) which was reported for MHD mixed convection flow of a centered conducting obstacle. The comparison is conducted while considering the dimensionless parameters $Ha = 10, 11$ and 12 and $Gr = 0.5, 0.8$ and 1.0 Present result for angle of inclination on flow velocity is shown in figure 2, which is in agreement with that of B.A Odongo *et.al* (2021). This justification gives the assurance in this numerical code under the stated objective.

5. RESULTS AND DISCUSSION.

In the current study, the Rayleigh number, Hartmann number, angle of inclination and the Absorption coefficient are varied within a constant Prandtl number $Pr = 0.71$. In this section, we consider the effect of Rayleigh and Hartmann number, angle of inclination on velocity profile components as well as the impact of Absorption coefficient on temperature profile. It is noted that both Hartmann and Rayleigh number, angle of inclination and absorption coefficient greatly affects the flow pattern. This therefore means that the aforementioned parameters affect the convective flow of the fluid and thereby affecting the movement of the centered conductor.

Effect of angle of inclination on horizontal fluid velocity profile

We hold constant the values of $Ra_T = 1000$, and solve equation (14) for values of varying values of ω . Table 1 shows horizontal fluid velocity with varying angle of inclination.

Table 1: Effect of angle of inclination on horizontal fluid velocity profile.

Angle of inclination	Chamber length, x(m)				
	0	1	2	3	4
$\omega = 45^\circ$	0.0712 35	0.0744 864	0.0750 436	0.0742555	0.0829442
$\omega = 60^\circ$	0.0740769	0.0811685	0.0830 311	0.0820422	0.0907568
$\omega = 90^\circ$	0.0755 57	0.0863766	0.0893757	0.0887995	0.0992755

Figure 2: Effect of angle of inclination on the horizontal velocity.

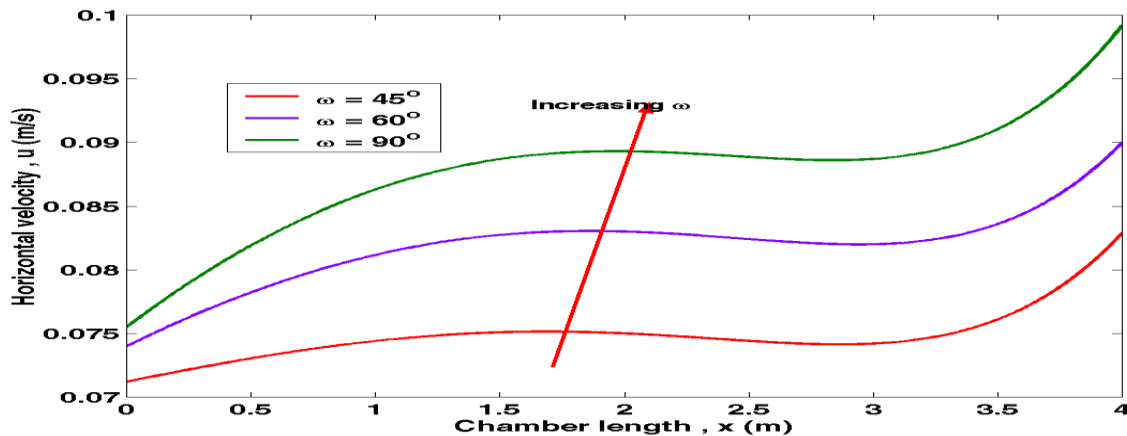


Figure 2 gives the influence of angle of inclination on the horizontal velocity profiles. It is observed that the velocity is increased steadily by increasing the angle of inclination. As indicated in the figure 2 below, the flow rate is at its maximum at $\omega = 90^\circ$ beyond this value, the velocity component of the flow drops exponentially to zero. Since the angle of inclination is a component of the force of buoyancy, the natural convective flow is high at $\omega = 90^\circ$. The fluid velocity is higher at the vertical surface than at the inclined surface since the buoyancy force acts normally on a body.

2. Effect of Rayleigh number on horizontal fluid velocity profile

We hold constant the values of $\omega = 45^\circ$ and solve equation (14) for values of varying values of

$Ra_T = 1000, 2000$ and 3000 in equation (8), we obtain the solutions of Ra_T as presented in the table 2.

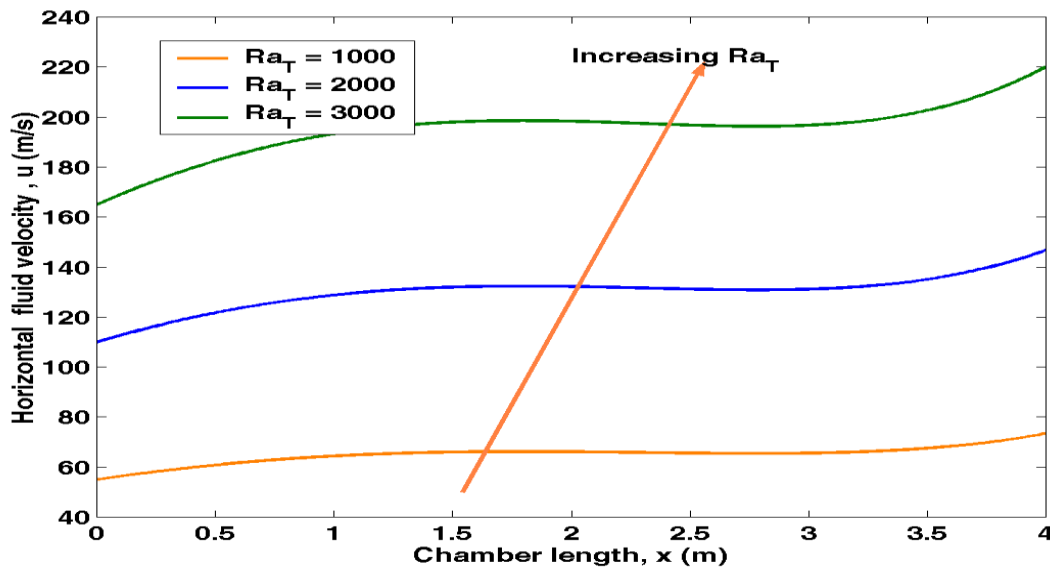
Table 2 shows horizontal fluid velocity with varying Rayleigh number.

Table 2: Effect of Rayleigh number on horizontal fluid velocity profile.

Rayleigh number	Chamber length, x				
	0	1	2	3	4
$Ra_T = 1000$	54.969867	64.39719864	66.10490750	65.56742555	73.35829483
$Ra_T = 2000$	109.9240769	128.786 853	132.200311	131.1230422	146.7075683
$Ra_T = 3000$	164.8767 57	193.1704766	198.293755	196.6797998	220.0527557

The results in table 2 are represented graphically as shown in figure 3.

Figure 3: Effects of Rayleigh number on horizontal velocity.



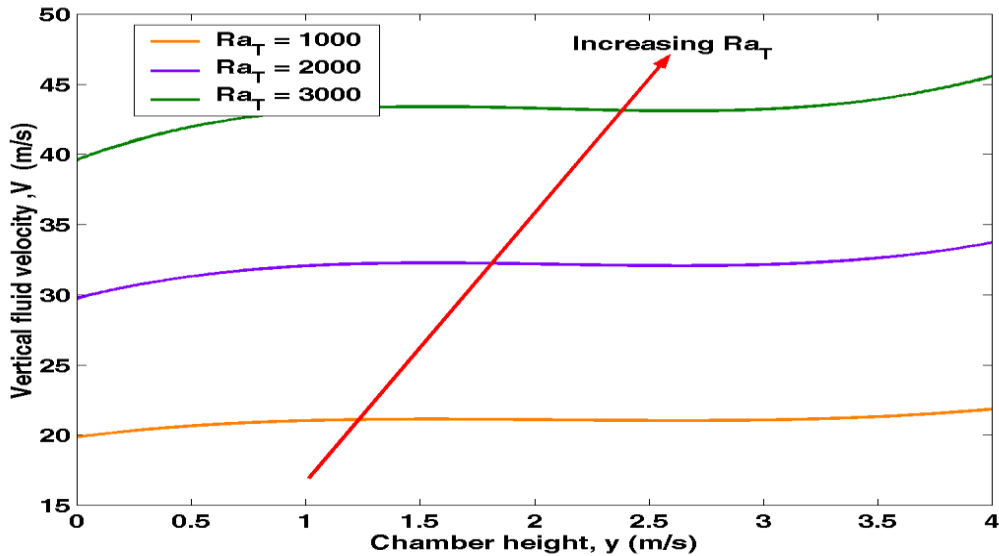
The effect of Rayleigh number on horizontal fluid velocity can be observed from figure 3. An increase in Rayleigh number leads to an increase in the horizontal fluid velocity. This is because the Rayleigh number is a product of force of buoyancy and thereby affecting the free convective part of this occurrence. The result also shows a conducting dominating regime is at low Rayleigh number with vertical velocity profiles since at low Rayleigh number below critical value, there is no fluid flow and heat flow is by conduction and a convective dominating regime is at high Rayleigh number with horizontal velocity profiles. At high Rayleigh number range, the fluid experiences turbulent flow thereby denoting an increased velocity profile.

3. Effect of Rayleigh number on vertical fluid velocity profile: We hold constant the values of $\omega = 45^\circ$ and solve equation (17) for values of varying values of $Ra_T = 1000, 2000$ and 3000 in equation (17), we obtain the solutions of Ra_T as presented in the table 3.

Table 3. Effect of Rayleigh number on vertical fluid velocity profile.

Rayleigh number	Chamber height, y(m)				
	0	1	2	3	4
$Ra_T = 1000$	19.87721432	21.031356494	21.099543722	21.077565	21.8573449
$Ra_T = 2000$	29.74487769	32.0595853	32.19609 311	32.1480422	33.711568
$Ra_T = 3000$	39.62095 57	43.08773766	43.29263757	43.220557995	45.5657758

Figure 4: Effects of Rayleigh number on vertical velocity.



From figure 4 above, it can be concluded that the strength of these vertical velocity profiles increases as the Rayleigh number (Ra) increases this is because Rayleigh number is a product of the buoyancy force. In addition, at high Rayleigh number, the fluid experiences turbulence flow which denotes an increased velocity. The result also shows a conducting dominating regime at low Rayleigh number with vertical velocity profiles and convective dominating regime at high Rayleigh number.

The results in Table 3 are represented graphically as shown graphically in figure 4

4. Effects of Hartmann number on vertical velocity profile

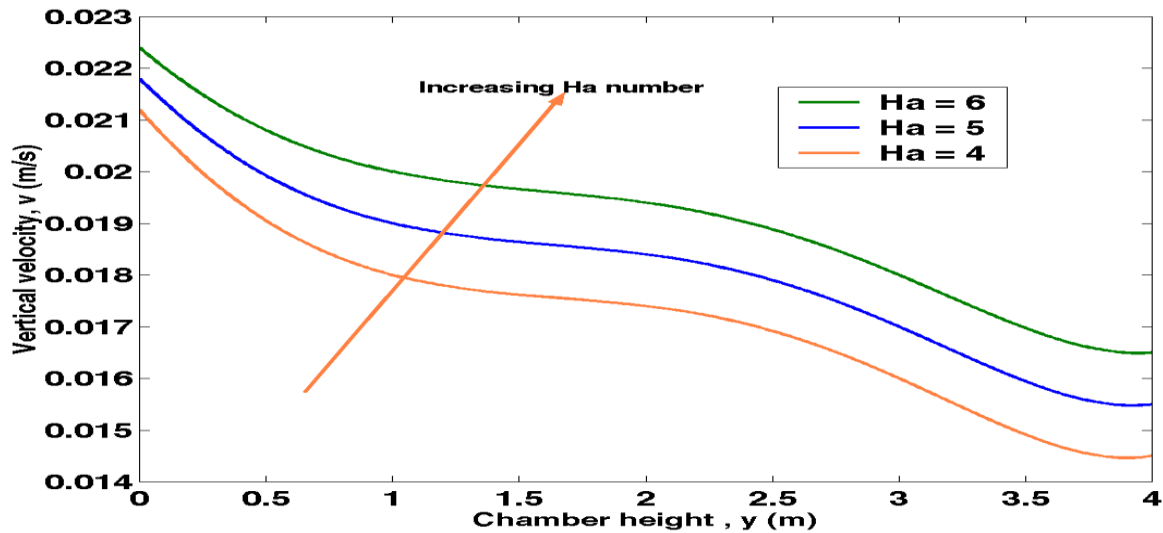
We hold constant the values of $Ra_T = 1000$, $\omega = 45^\circ$ and solve equation (17) for values of varying values of $Ha = 4, 5$ and 6 in equation (17), for varying values of Ha , we obtain solutions as presented in the table 4 below.

Table 4. Vertical fluid velocity with varying Hartmann number

Hartman number	Chamber height, y(m)				
	0	1	2	3	4
$Ha = 4$	0.02242373	0.02008426	0.01942971	0.018014275	0.01652252
$Ha = 5$	0.02183564	0.01907728	0.01840992	0.017035289	0.01552758
$Ha = 6$	0.0212922	0.01806648	0.017411235	0.01605638	0.01456488

The results in table 4 are represented graphically as in figure 5 below;

Figure 5. Vertical velocity against chamber length with varying the Hartman number.



From the above, it can be concluded that the velocity is influenced by Hartmann number which is a product of the induced Lorentz force. This is due to the formation of a narrower boundary zone, which shows a general trend to induce an electromotive force to the free stream flow of MHD, hence the velocity reduces as shown above. The Lorentz force induced as a result of electrically conducting fluid flow acts against the flow for an applied magnetic field acting in the normal direction as in the current problem. The opposition created lowers the velocity of flow and thereby affecting the general convective current.

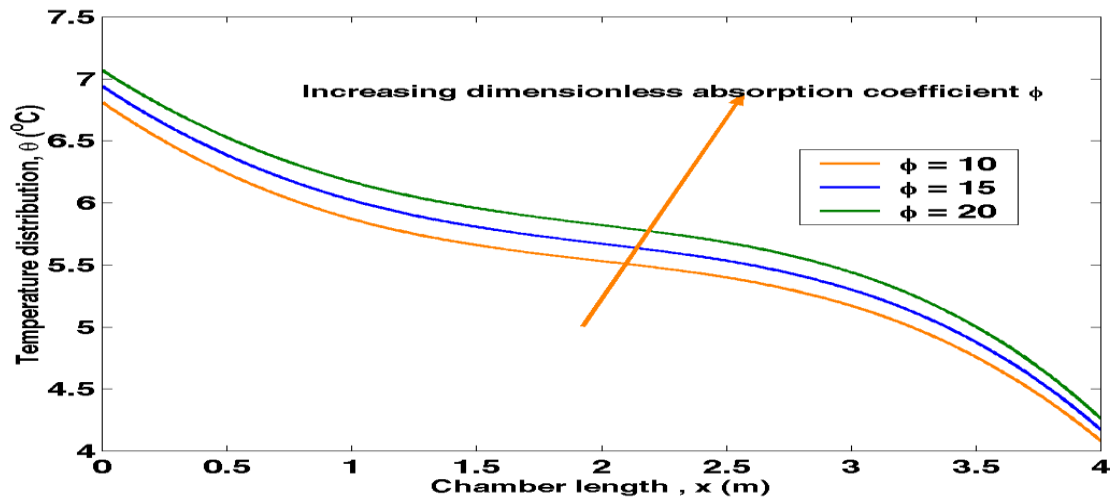
5. Effect of dimensionless absorption coefficient on temperature distribution

We varying $\Phi = 10, 15,$ and 20 in equation (20). Solving equation (20) for varying values of Φ , we obtain solutions for varying Φ as presented in the table 5 below.

Table 5. Fluid temperature distribution for varying dimensionless absorption coefficient.

Dimensionless absorption coefficient	Chamber length, x				
	0	1	2	3	4
$\Phi = 10$	6.813856	5.872194	5.5395637	5.1702643	4.0835628
$\Phi = 15$	6.941472	6.021216	5.6722278	5.3011632	4.172579
$\Phi = 20$	7.069552	6.170012	5.823442	5.4426483	4.263325

Figure 6 .Temperature against chamber length with varying dimensionless absorption coefficient:



In the figure.6 above,it can be concluded that for certain values of dimensionless absorption coefficient, the surface heat flow tends to decrease by increasing in Φ . This in turn affects the density variation between colder and hotter parts of the fluid. At higher values of Φ , the surface heat transfer or the temperature difference (thermodynamic driving force) tends to decrease thereby lowering the velocity of the flow.

The above parameters discussed, strongly affect the fluid flow components which is in agreement with study's objective.

6. CONCLUSION

A numerical study performed to analyze the influence of the effects; Rayleigh number,

Hartmann number, angle of inclination, and absorption coefficient on fluid velocity profiles

and temperature distribution. The following outcomes can be deduced from the study:

- An increase in Rayleigh number increases the buoyancy force thereby raising the fluid velocity rate.
- . An increase in absorption coefficient lowers the surface heat flow (density variation due to temperature change). Thereby lowering the fluid flow rate.
- The angle of inclination of a conductor directly affects the buoyancy force component, thereby affecting the rate of fluid flow. The buoyancy force increases with an increase in angle of inclination. This factor has an impact on flow rate within a given range values discussed above.
- An increase in Hartmann number lowers the flow rate of fluid. This is due an increase in Lorentz force formed which causes an opposite force to the flow.

The said findings can be applied in the field of engineering to improve the flow rate of MHD fluids and their extensive application.

Conflicts of interest.

We do declare that there is no conflict of interest regarding the publication of this

research paper. Therefore the paper can be published.

REFERENCES.

- 1) Nasrin,R. (2011).Influence of a centred conducting obstacle on MHD Mixed convection in a wavy chamber. The Journal of Naval and Marine Engineering. **8 (2)**.
- 2) Moreau *et.al.* (1992). Natural convection in a rectangular cavity with a horizontal magnetic field. International Journal of heat mass transfer. (**35**), pp 740 – 747.
- 3) Sigey*et.al* (2013). Magneto hydro-dynamic free convective flow past an infinite vertical porous plate with joule heating. Applied Mathematics. (**4**.)
- 4) Patankar, S.V. (2004). Numerical heat transfer and fluid flow. Hemisphere publishing corporation USA.
- 5) Oztop *et.al.* (2016).Mixed convection of nano – fluid filled cavity with oscillating lid under the influence of an inclined magnetic field. Journal of the Taiwan Institute of chemical Engineers **63**.Pp 200 -225.
- 6) Karimipour *et.al.* (2020). Magnetic field influenced on combined convection heat flow in a lid – driven rectangular enclosure. Journal of Akademia Baru. (**12**), pp 13 – 21.
- 7) Mahdy*et.al.* (2013).MHD combined convection in a tilted lid – driven enclosure with opposing thermal buoyancy force: Influence of non – uniform heating on both side walls. Nuclear Engineering and Design **265**. Pp931 – 949.
- 8) Roy S. and Basak T. (2005). Finite Element Analysis of free convection flow in a square enclosure with differently heated walls. International journal of Engineering Science.

pp 668 -680.

9. Sagheer M., Mehmood K. and Hussain S. (2010). MHD combined convection and entropy generation of water alumina nano fluid flow in a double lid driven enclosure with discrete heating. *Journal of Magnetism and Magnetic Materials* **419**.

pp 140 – 155.

10. Sarris I.E., Kakarantzas S.C., Grecos A.P. and Vlachos N.S. (2005). MHD natural convection in a sideways and volumetrically heated square cavity. *International Journal of Heat and Mass Transfer* **48**, pp3443 – 3453.

11. Sigey J.K., Okelo J.A., Ngesa J. and Gatheri K. (2013). Magneto hydrodynamic free convective flow past an infinite vertical

porous plate with joule heating. *Applied mathematics*. **4**

12. Singh A.K. (2002). Numerical solution of hydro magnetic non-steady natural convection flow past an infinite permeable plate. *Indian journal of Pure and Applied Physics* **41(3)**. Pp 167 – 170.

12. Smith T.F., House J. and Beckermann C. (1990). Effects of a centered conducting body on natural convection heat transfer in an enclosure. *Numerical heat transfer. Part A*. **18**, pp21 -25.

13. Sharqawy M.H., Zubair S.M. (2010). *Thermophysical properties of sea water*.

Author profile.



Mr. Samson Juma holds Bachelor of Education Science with IT degree in Mathematics and physics with Second class honors from Maseno University, Kenya. At the moment, he is pursuing Masters of Science in Applied Mathematics at Jomo Kenyatta University of Agriculture and Technology. He is a full-time teacher at Othoro secondary school, Kenya. He has much interest in the study of fluid mechanics and their corresponding applications in science and engineering.



Prof. Johana Sigey, holds Bachelor of science degree in mathematics and computer science first class honors, Masters of science degree in Applied Mathematics from Kenyatta University and a PhD in Applied Mathematics from Jomo Kenyatta University of Agriculture and Technology, Kenya. Currently he is a Professor Department of Pure and Applied Mathematics at Jomo Kenyatta University of Agriculture and Technology. He has published 56 papers on Heat transfer in respected journals.



Prof. Jeconia Abonyo, holds a PhD in Applied Mathematics from Jomo Kenyatta University of Agriculture and Technology alongside Masters of science degree in Mathematics and first class honors in Bachelor of Education, science; Mathematics and Physics option both from Kenyatta University. Currently, he is serving as a professor Department of Pure and Applied Mathematics at Jomo Kenyatta University of Agriculture and Technology. He has 54 publications on heat transfer with respected journals.



Dr. Simeon Maritim, holds PhD in Applied Mathematics from Eldoret University as well as a Master's of science in Applied Mathematics and a Bachelor of Education degree both from Kenyatta University. He also holds a diploma in Education from Kenya Science Teachers College. Currently he is a senior lecturer Department of Mathematics and Computer science at Bomet University College. He has 6 publications in Applied Mathematics with respected journal.